UCLA
COMPUTATIONAL AND APPLIED MATHEMATICS

The Vortex Ring Merger Problem at Infinite Reynolds Number

Christopher Anderson
Claude Greengard

November 1988

CAM Report 88-35

Department of Mathematics
University of California, Los Angeles
Los Angeles, CA. 90024-1555

The Vortex Ring Merger Problem at Infinite Reynolds Number

CHRISTOPHER ANDERSON
University of California at Los Angeles

CLAUDE GREENGARD
Courant Institute and IBM T.J. Watson Research Center

1 Introduction

The physics of three-dimensional incompressible fluid flow, as is well known, is an extremely difficult and not well understood subject. The mathematical theory of the Navier-Stokes and the Euler equations is incomplete and a detailed qualitative understanding of the dynamics is, for the most part, lacking.

One focus of recent research which aims at an understanding of key features of turbulence and of the possible breakdown in regularity of solutions of the fluid equations has been on the motion of vortex filaments [10], [19]. Motivations for the study of vortex filaments are the prevalence of thin vortex tubes in experimentally observed flows, the fact that the Euler equations can be thought of as an evolution equation for a continuum of interacting vortex filaments, and a view of turbulence as being characterized by wildly stretching and dissipating vortex filaments.

A vortex flow problem which has been the subject of interesting laboratory and numerical experiments is the vortex ring merger problem. In this problem the evolution over a short interval of time of two initially parallel (or slightly inclined) co-rotating

vortex rings of the same strength is studied. The rings are observed to come together and "reconnect," in the sense that much of the vorticity field becomes composed of vortex lines which join the two initially distinct vortex rings. This merger occurs on a timescale which is much shorter than that expected from a simple dimensional analysis based on the magnitude of viscosity and on the vortex ring radius [3].

The numerical computations which are reported in this paper give approximations to the vortex ring merger flow in an inviscid (infinite Reynolds number) fluid. Since vortex lines are preserved in time for inviscid, incompressible flow, there can be no ring merger in our calculations. However, much insight can be gained into the nature of ring merger from properties of the solution of the inviscid problem. In particular, it can be seen from our calculations why reconnection occurs as rapidly as is observed, and why reconnection can be expected at even extremely high values of the Reynolds number.

Of perhaps more fundamental interest is the light these calculations shed on conjectures about the possible development of singularities in Navier-Stokes and in Euler flow, and on models of energy cascades and the generation of small spatial scales in turbulence theory. As we observe in our calculations, the vortex rings approach each other very closely, and the vortex cores which form the adjacent edges of the two rings undergo severe strain imposed by the vorticity which forms the outer portions of the rings. This strain consists of an extremely rapid axial flow along the vortex cores and of a severe contraction in one, but not the other, direction orthogonal to the axis of the vortex tube. The result is two very close, very thin, vortex sheets.

As we argue in the concluding section of this paper, the evolution of the vortex cores into vortex sheets suggests that the vortex stretching will be bounded and that

flows such as that examined here do not provide a mechanism for the breakdown of smooth solutions of the Euler equations. The transformation of cylindrical cores into vortex sheets which we have observed may be of interest in connection with theories of the inertial range of turbulence, for this evolution suggests a new scenario for the transfer to small spatial scales of parts of the vorticity field and for the possibility of rapid removal of this vorticity by the action of viscosity. This issue is also discussed at greater length below.

The numerical scheme we have employed is a vortex filament method. We are tackling an inviscid problem with an inviscid scheme. The scheme is inviscid in the sense that there is no accumulation of numerical diffusion and extremely small spatial scales can be resolved since the computational elements are Lagrangian and are not tied to fixed, regular positions in space. These two properties, which permit the calculation of very thin structures in the flow, are crucial for the success of this investigation.

In the remainder of this paper, we introduce the vortex method we have implemented and show that it gives a proper discretization of the Euler equations (in Section 2). In Section 3, we discuss the results of some of the numerical experiments we carried out. Section 4 contains our conclusions.

2 The Numerical Method

Ideal fluid motion preserves vortex filaments and their circulations. Moreover, the velocity field is uniquely determined by the distribution of vorticity (because of incompressibility). Consequently, the evolution of an ideal fluid can be described in terms of the evolution of its vortex filaments alone.

The algorithm used in the computations described in this paper involves the dis-

cretization of vortex rings into finite numbers of vortex filaments and the discretization of each filament into a finite number of particles. (See [15] for a general discussion of three-dimensional vortex methods.) The vorticity is represented by a finite set of vectors of vorticity located at the midpoints of the segments which join neighboring particle pairs and of length and orientation determined by the separation of the neighboring particles [9]. The velocity contributions at the particle positions due the discrete vorticity field are added to give the velocity of each particle, and the evolution in time of the collection of vortex filaments is thus computed.

Before describing in more detail the vortex method we have implemented, we pause to present the equations of motion for a vortex ring in terms of the vortex filaments. Our algorithm is a straightforward numerical approximation of this system of equations. We assume for the present discussion that the initial distribution of vorticity consists of a single vortex ring; the extension to the case of several vortex rings is obvious. Let B be a two-dimensional disk, which we identify with a ring cross-section, and let $\xi : B \to \mathbf{R}$ give the vortex strength in each cross section. We assume that ξ has only radial dependence and is zero at the boundary of B. We parameterize the vortex ring $A \subset \mathbf{R}^3$ of radius R by the map $X : B \times [0, 2\pi] \to A$, given by setting

$$X(b, \phi) = ((R + b_1)\cos(\phi), (R + b_1)\sin(\phi), b_2),$$

where $b = (b_1, b_2)$, and assume that the initial vorticity distribution $\omega(\cdot, 0)$ is given by

$$\omega(X(b, \phi), 0) = \xi(b)(\cos(\phi), \sin(\phi), 0).$$

In this way, the images under X of the "circles" $\{(b, \phi) : 0 \leq \phi \leq 2\pi\}$, with $b \epsilon B$ fixed, are vortex filaments in the ring.

We denote positions within the initial ring configuration by $\alpha \epsilon A$ (these are our

Lagrangian coordinates) and describe trajectories of fluid particles by letting $\Phi_\alpha(t)$ denote the position at time t of the fluid particle which at time 0 was located at the spatial position α. The conservation of circulation implies that the vorticity $\omega_\alpha(t) = \omega(\Phi_\alpha(t), t)$ is determined from its initial value and the deformation of the fluid through the relation (setting $(b, \phi) = X^{-1}(\alpha)$)

$$\omega_\alpha(t) = \xi(b) \frac{\frac{\partial(\Phi \circ X)}{\partial \phi}(b, \phi)}{|\frac{\partial X}{\partial \phi}(b, \phi)|} = \frac{\xi(b) \frac{\partial(\Phi \circ X)}{\partial \phi}}{R + b_1} \tag{2.1}$$

(see [12]). The velocity $u(x, t)$ at spatial position x and time t is given from the Biot-Savart formula by

$$u(x, t) = \int_A K(x - \Phi_\alpha(t)) \omega_\alpha(t) d\alpha, \tag{2.2}$$

where K is the operator $\frac{x}{|x|^3} \times$. Making use of (2.1)-(2.2), we can write the equations of motion of the ring in the form

$$\Phi_\alpha(0) = \alpha \tag{2.3}$$

$$\frac{d}{dt} \Phi_\alpha(t) = \int_A K(\Phi_\alpha(t) - \Phi_\beta(t)) \omega_\beta(t) d\beta. \tag{2.4}$$

The system (2.1),(2.3)-(2.4) is equivalent to Euler's equations.

We discretize the equations of motion (2.1),(2.3)-(2.4) by approximating the vorticity by Lagrangian finite differences and the integral in (2.4) by the trapezoidal rule. Let $m > 0$ be an integer and set $h = 2\pi/m$. We will refer to two grids on $B \times [0, 2\pi]$ of mesh width h. These are the grids $\{(k_1, k_2, k_3)h\}$ and $\{(k_1, k_2, k_3 + 1/2)h\}$ ranging over the three-tuples of integers (k_1, k_2, k_3) such that $(k_1, k_2)h \epsilon B$ and $0 \leq k_3 < m$. We denote by $\{\tilde{\alpha}_i\}$ and $\{\tilde{\alpha}_i^+\}$, respectively, the two sets of grid points, and by $\{\alpha_i = X(\tilde{\alpha}_i)\}$ and $\{\alpha_i^+ = X(\tilde{\alpha}_i^+)\}$ the corresponding sets of curvilinear grid points in the initial vortex ring. (See Figure 1.)

Let $x_i(t)$ denote our computational approximation to $\Phi_{\alpha_i}(t)$. Assume that α_i and α_{i+1} are adjacent grid points along one of the initial discrete filaments and call α_i^+ the shifted grid point between these two. Then $m_i(t) = (x_{i+1}(t) + x_i(t))/2$ and $\tilde{\omega}_i(t) = \frac{x_{i+1}(t) - x_i(t)}{(R + b_1)h}\xi(b)$ (where b is the cross-sectional coordinate of the filament in question) are approximations to $\Phi_{\alpha_i^+}(t)$ and $\omega_{\alpha_i^+}(t)$ (see (2.1)), respectively. Denote by b^i the cross-sectional coordinate of α_i. A velocity field $\tilde{u}$ which approximates u can now be defined by the following discretization of (2.2):

$$\tilde{u}(x,t) = \sum_i K_\epsilon(x - m_i(t))\tilde{\omega}_i(t)h^3(R + b_1^i) \ , \tag{2.5}$$

with the summation including all of the grid points. K_ϵ is an approximation to K obtained by the convolution of K with a cutoff function $K_\epsilon = K * \phi_\epsilon$, where $\phi_\epsilon(x) = \epsilon^{-3}\phi(x/\epsilon)$ and where we use the function

$$\phi(x) = \begin{cases} \dfrac{3}{4\pi} & \text{if } |x| \leq 1 \\ 0 & \text{if } |x| > 1 \end{cases} \ ,$$

for which the convolution can be carried out explicitly (without need for a numerical integration). The final factor in (2.5) is due to the transformation from the cubic to the curvilinear grid and is needed to make the summation a correct approximation to the integral over A. Observe that, setting $\omega_i(t) = \xi(b)(x_{i+1}(t) - x_i(t))/h$, we can rewrite (2.5) in the form

$$\tilde{u}(x,t) = \sum_i K_\epsilon(x - m_i(t))\omega_i(t)h^3 \ . \tag{2.6}$$

With the above approximation to the velocity assumed, the system of ordinary differential equations governing the evolution of discrete filaments is given by

$$x_i(0) = \alpha_i \tag{2.7}$$

$$\frac{dx_i}{dt}(t) \;=\; \sum_j K_\epsilon(x_i(t) - m_j(t))\omega_j(t)h^3, \tag{2.8}$$

with i and j ranging over all the grid points. The m_i and ω_i are determined by the x_i as above. The discretization in time of this ordinary differential equation constitutes our algorithm. This algorithm is a lower order version of the one whose convergence was proved in [12], following the works [2] and [7], [8].

In all but the simplest flows, a great amount of vortex stretching occurs, and in order to resolve the flow adequately, it is necessary to add computational elements as the calculation proceeds. At each time step, we check the distances between neighboring particles on the discrete filaments. When a threshold value is exceeded, we include a new particle between the original pair. This new particle is placed at the midpoint of the two particles. The nature of the algorithm is such that the vorticity used in the computation of the velocity can be evaluated as before. In general, in regions of significant stretching, many new particles are added between two originally neighboring particles. It is in order to obtain a reasonably accurate interpolation procedure that we have used the algorithm described above, rather than the higher order one described in [12].

Numerical resolution is improved as the number of particles tends to infinity ($h \to 0$), the smoothing parameter ϵ tends to zero, and the timestep in the discretization of the ordinary differential equations tends to zero. The order in which the limiting procedures, $\epsilon \to 0$, $h \to 0$, are carried out is important. If one fixes h and lets ϵ tend to zero, the calculations easily become unstable because of the singularity of the Biot-Savart kernel. The convergence theory requires that the smoothing parameter should be of higher order than the original interparticle mesh spacing. If one sets $\epsilon = h^\gamma$, with $\gamma < 1$, then one can obtain convergence as h decreases to zero. However, in practice

are investigating would be destroyed by even tiny amounts of diffusion, this non-diffuse feature of the approximation is crucial to the success of our calculations. Furthermore, the non-diffusive character is present for all ε, and the method should provide reliable insight as to the qualitative features of the solutions of Euler equations, even for relatively large values of the smoothing parameter.

Some final comments we would like to make about the numerical algorithm concern the objections which are sometimes raised that the computational vorticity field is not divergence-free in the vortex method. First and foremost, one can answer such objections by observing that numerical algorithms should give good approximations to the continuous problem; they need not provide exact solutions of discretized forms of physical laws. Calculations of fluid flows by the finite element method are not faulted because velocity fields in real fluids are not affine functions on triangles in space. Secondly, as has been observed by Beale [4], the curl of the velocity field induced by a collection of vortex elements of the type considered in this paper is the projection of this vorticity field onto the space of divergence-free vector fields. Thus, the velocity field induced by our vortex elements is identical to that induced by a vortex distribution which is divergence-free.

3 The Numerical Results

As initial conditions, we took two identical, axisymmetric vortex rings. We studied the evolution of these rings over a short interval of time, though one long enough for the rings to come together, for the vortex cores to become severely distorted, and for the rings to begin to pull apart in the direction orthogonal to that joining the two rings.

The initial distribution of vorticity is determined by the radius ρ_R of the rings, the cross-sectional radius ρ_C, the vorticity distribution function ξ (see Section 2), the separation ρ_S of the ring centers, and the initial angle of inclination of the rings to the (x, y)-plane. We choose the coordinate axes so that the ring centers are equidistant from the origin on the x-axis, at the positions $c_+ = (\rho_s/2, 0, 0)$ and $c_- = -c_+$. The rings were taken to be inclined toward one another by 20^o. Qualitatively similar evolution results from initially coplanar rings, but the interesting interaction occurs sooner when the rings are inclined from the beginning, and so a higher proportion of the computational labor can be used to resolve the interaction process. Figure 2 illustrates the initial configuration of the vortex rings.

We chose the initial cross-section to be uniform, with ξ the (scaled) characteristic function of the ring. The scaling was chosen so that the circulation of each ring is 20. In all of the computations reported here the vortex ring parameters were taken to be $\rho_R = .1$, $\rho_C = .02$ and $\rho_S = .25$. Again, qualitatively similar evolution is observed when the uniform cores of vorticity are replaced by a more smoothly varying vorticity distribution.

Some of the features of the evolution of the vortex rings, starting from the given initial conditions, can be seen in the perspective views of Figures 3(a)–3(d). These figures show the positions of a few of the 61 filaments which make up each ring at steps 16,32,48 and 64 (the vortex rings would be solid black if all of the filaments were plotted.) The plots are in a frame of reference moving with the center of mass of the vorticity; one should keep in mind that the rings are translating downward, even though the rings remain in the center of each frame. These figures were obtained with the parameter $\delta = .012$ and the number of computational particles $N = 5490$ initially

and $N = 6148$ at the final time.

For those readers who are not well acquainted with the ring merger problem, even the basic features of the flow can be obscure and not easily discernible from the pictures. A very helpful description can be found in [18]. For the benefit of the reader, we attempt a brief description of the movement of the rings in the next paragraph.

For an individual ring, the velocity field which it induces upon itself is close to being a sum of a uniformly downward velocity and a rotation about the core. Thus, as the rings in our computation are initially inclined, each one has a component of velocity which induces a translation downward and toward the other. The effect of one ring is to retard the downward motion of the other, especially at the nearby side. As the tilt of the rings is increased, the component of the self-induced velocity in the direction joining the rings is increased, and the rings approach each other and press together. The velocity field due to the vorticity in the near edges of the two rings (which are almost tangent to one another and contain vorticity of opposite sign) is negligible except very near these edges. The motion induced by the edges upon one another, however, is non-negligible—each edge imparts an upward component of velocity to the other. In pressing against one another, the portion of each ring which is nearest to the other becomes stretched and flattened. This is seen in Figure 3(d) which is the ring at the final time of the computation.

Of primary interest, as we discuss in the next section, is the structure of the core of the rings in the region where the rings come closest together. In figures 4(a) - 4(d) cross-sectional views of the rings at the times corresponding to those in Figures 3(a)-3(d) are presented. Here the intersections of the computational filaments with the (x, z)-plane are plotted. As is clear from these plots there is significant flattening

of the vortex cores as they come close together. The incompressibility of the flow and the diminishment of the core sizes implies that a great amount of stretching of the vorticity, in the directional normal to the cross-sections, is taking place.

In order to quantify the flattening we computed the average of the x-coordinate separation of the points which make up Figure 4. This gives an estimate of how close the two cross-sections are pushed together. The ratio of this average distance of separation with the original average separation is plotted as the solid line in Figure 5(a). The cross-sectional area was measured, and the dashed line Figure 5(a) is the ratio of the cross-sectional area of the tube to the original cross-sectional area. The decrease in cross-sectional area indicates that a large amount of stretching of the tube has occurred. The magnitude of this stretching is indicated In Figure 5(b) were we plot the maximum stretching and the average stretching for the vorticity on the cross-sectional slice. The implications of these results will be discussed in the next section, but we now address the establishment of the reliability of the computed results.

In our computations we choose h sufficiently small so that for the given δ the changes in the solution were negligible. Of more importance are the changes in the solution with respect to the smoothing parameter δ. In order to assess this we computed the evolution of the rings with several different values of the smoothing parameter and compared the results.

We focus our attention now on three different values, $\delta = .015$, .012, and .010. Our first observation was that the overall development of the rings was essentially independent of δ, *i.e.* views of the type in Figures 3(a)–3(d) do not differ substantially among the different values of δ. Significant differences, however, are found in the behavior of the core cross-section at the points where the two rings come closest

together. In Figure 6 we plot the cross-sections of the filaments with the x-z plane at steps 16, 32, 48 and 64 for the three different values of δ. The number of particles N at the beginning of the computation was the same — 3904. The results for a given value of δ are in a single column, and the size of δ decreases as one goes left to right. It is clear from these pictures that the solutions have not converged with respect to δ, but a trend can be clearly seen. Notably, there is tremendous flattening at all values of δ and the major difference is in the structure at the top of the cross-section. As δ decreases, this structure appears to become more flattened.

The behavior of the average cross-sectional separation is plotted in Figure 7. For the early part of the computation, the results agree rather well, while near the end they differ. For the three values shown, the figures indicate that the separation distance are decreasing as δ is decreased. A similar trend is observed in the cross-sectional area.

In our computational results we see that there is tremendous deformation of the core in the region in which the two rings press together. We have not computed solutions which are completely independent of δ, but the results suggest that we have captured the essential features of the solutions. In fact, the deformation which we observe appears to be more pronounced as the smoothing parameter is reduced.

4 Implications for Fluid Mechanics

The vortex ring interaction which we have investigated, and described in this paper, is a particular example of an important class of vortex flows. Although the initial conditions appear to be very special, the striking core deformations which we have observed are relevant to other investigations of vortex dynamics. In this section we discuss the implications of our results concerning questions about the appearance of

singularities in finite time, the vortex dynamics of the inertial range, and the nature of ring merger or reconnection in viscous flows.

Three-dimensional vortex dynamics seems to be characterized, in part, by the pairing of anti-parallel pieces of vortex tubes. This phenomenon has been observed in numerical experiments [19] and can be expected in the presence of substantial vortex stretching from the invariance of the energy $\int \omega(\mathbf{x}) \cdot \omega(\mathbf{y})/|\mathbf{x}-\mathbf{y}| d\mathbf{x}d\mathbf{y}$ (here ω is the vorticity and the integration is over all space). In the pairing process, substantial stretching and very close approach of the pair of tubes occurs.

The authors of [19] and [20] presented evidence which, they argued, suggests that the stretching which takes place when pairs of vortex tubes come together may become infinite after a short time, leading to singularities in solutions of the Euler equations (or even the Navier-Stokes equations). In the calculations presented by these authors, two oppositely signed vortex filaments come together, "pair", and translate rapidly. This translation induces local stretching which further enhances the velocity of translation and consequent stretching, and the stretching becomes infinite after a short time. However, the vortex cores are resolved by single filaments and so by necessity these cores are always circular. As we see from our numerical results, notably Figures 4(c)–4(d), the core shapes differ dramatically from circles. This fact has important consequences for the possible development of singularities.

To understand the relevance of the cores shapes, imagine a model in which two identical tubes of vorticity (by which we mean a bundle of filaments), of opposite circulation, traveling towards each other, each being moved by an externally imposed velocity (which in the case of our problem is due to the vortex ring configurations). As they begin to approach one another, each acts on the other as well. Take the tubes to

be orthogonal to the (x, z)-plane at the point where they come closest together, with the cross-sectional centers of each on opposite sides of the origin along the x-axis. The amplification of the vorticity due to stretching has minimal immediate effect on the dynamics of the cores, because the circulation in the (x, z)-plane is independent of the stretching. However, the compression in the plane, which of necessity accompanies stretching (because of incompressibility), has a major effect on the velocities induced by the cores. If there is compression in the z-direction as well as in the x-direction, then as the cores approach each other, the induced velocities increase rapidly, being of order $|x|^{-1}$, and one could expect catastrophic behavior. This is the beginning of the approach to singularity seen in [19]. However, if there is contraction only in the x-direction, then the cores begin to resemble vortex sheets, and the greater the flattening, the weaker are the sheet strengths. The velocities induced by vortex sheets on each other remain bounded. Our results show that, indeed, a severe flattening takes place — the cores are smashed into sheets and in effect lose a dimension. Thus, the capability of the vortex tubes to feed on each other nonlinearly until blow-up seems not to be present in our problem. A necessary condition for a singularity to occur is an infinite stretching of a part of a vortex line [5]. Of course, we do not claim that the flow is nonsingular for all time, only that the kind of singularity described earlier does not seem to occur here. (The description of the tubes coming together we have given assumes that they are of identical strength and symmetrically placed with respect to one another, which is also the assumption made in the numerical calculations of others to which we have referred. It is important to observe that, although we have presumably excluded the generic cases in this way, we have considered a more singular situation, for if the cores are not of the same strength, then the weaker one will begin to

wrap around the stronger one, resulting in even more two-dimensional core distortion as well as increased vorticity cancellation, and thus less wild stretching. Also, as indicated by the numerical calculations of Melander and Zabusky [16] on the motion of anti-parallel vortex tubes, significant core distortion and rapid cancellation can be expected if the rings are not in a symmetric configuration.)

It should be mentioned that Pumir and Kerr [17] have previously shown (at finite Reynolds number) that some deformation of the cores takes place in the flow, raising questions about the blow-up picture, but the deformation was sufficiently mild as to leave open the question of how singular the induce velocities may be becoming.

The core deformation which we have observed may also be of considerable interest in connection with certain aspects of turbulence theory. Chorin [11] has pointed out that folding and pairing of vortex lines is necessary, in the presence of stretching, in order that energy be conserved, and has suggested that a study of the kinds of folding and pairing which may occur is of great value to the understanding of three-dimensional vortex dynamics and the inertial range of turbulence. The passage to smaller scales in this picture is brought about by the stretching of the vortex lines. Our work reveals another, contemporaneous, process for generation of small spatial scales — vortex tubes can squash into vortex sheets as they stretch, and in this way bring about much smaller spatial scales of vorticity than would be predicted by the value of the rate of stretching of the vortex filaments alone.

In order to study vortex dynamics and the passage to small scales, without having to carry out the impossible task of doing accurate, very high Reynolds number, fairly long time three-dimensional calculations, Chorin [11] has made a lattice model (or "cartoon," to use Chorin's term) of vortex dynamics in order to study energy cascades

and the inertial range of turbulence. It appears to us that a model of vortex core flattening could be reasonably incorporated into Chorin's lattice model.

The final issue we address is the nature of the vortex ring interaction in the presence of a small amount of viscosity. The viscous flow is of great current interest, principally because of the beautiful experiments which have been carried out showing what is called vortex ring reconnection or merger (beginning with Kambe and Takao [13] and most recently by Schatzle [18]). Our calculations have been carried out at infinite Reynolds number and the question of the relation between our results and those of slightly viscous flows is of interest.

As long as the inviscid flow is smooth (as appears to be the case here), solutions of the Navier-Stokes equations converge to the inviscid flow as the viscosity tends to zero [6]. It is clear that while the two vortex rings are well apart from one another, the effect of a small amount of viscosity will be negligible. If one considers a cylindrical tube of vorticity with the same circulation and diameter as the tubes which make up the rings in our computation, then above Reynolds number 6,500 the vorticity diffuses a mean distance less than one percent of the core diameter by time step 64 (the final time in our computation). What is of more interest is when the rings are close together. As our calculations reveal (most notably in Figure 4(d)), portions of oppositely signed vorticity get flattened together and even quite small amounts of viscosity will lead to a cancellation of the vorticity. This explains why reconnection occurs at a rapid rate for the viscous problem, even at high Reynolds numbers. The tendency for flattening has been observed in the viscous calculations in [17].

Also related to the issue of the approximation of the inviscid flow by a viscous one is the nature of the merger process. Since vortex lines are not broken for the

inviscid flows merger cannot occur. In the viscous case it does occur and therefore, there has been some controversy about the nature of the inviscid limit. Above some Reynolds number is there no reconnection? Or is the limit discontinuous (in the sense of vortex reconnection) as the Reynolds number tends to infinity? One source of this controversy has been the fact that reconnection has not been well defined. For all arbitrarily small positive times and values of viscosity, there exist vortex loops which cross the plane of symmetry (the (y-z) plane in our calculation). A proper definition of reconnection should specify some further condition on such loops. Let us denote by $\mathbf{x}(\alpha, t)$ the position at time t of the fluid particle which at time 0 was located at position α. One could define the time of reconnection to be the first time t such that for some α which lies in one of the initial vortex rings, the vortex line through $\mathbf{x}(\alpha, t)$ crosses the plane of symmetry. One could also ask for the first time T when, say, one half of the original vorticity-carrying part of the fluid lies on such vortex lines. With these definitions, it is clear that there exists a critical Reynolds number R_T such that in $[0, T]$, solutions for Reynolds numbers $R > R_T$ experience no reconnection, while those corresponding to $R < R_T$ do. Thus reconnection does not occur above a finite Reynolds number, and the limit is nonsingular.

In summary, we have presented the results of a computation of the interaction of two vortex rings. This problem appears to be a good model of more general interactions of vortex tubes. We have investigated the solution of the inviscid equations, a problem which to our knowledge has not previously been attempted with fully three-dimensional vortex cores. We have seen that the cores flatten severely as they smash into each other. Although a tremendous increase in the magnitude of vorticity is observed, the computational evidence shows that due to the evolution of the vorticity into sheets, this

does not lead to large velocities and hence a catastrophic intensification of vorticity. In fact, the evidence suggests that the velocity remains bounded and the magnitude of the vorticity only grows linearly with time. There is also evidence of a new process for the generation of small spatial scales which may be of importance in the inertial range of turbulence.

Acknowledgements. Research of the first author was supported in part by ONR Contracts N00014-86-K-0727, N00014-86-K-0691 and NSF grant DM586-57663. Research of the second author was supported in part by a National Science Foundation Mathematical Sciences Postdoctoral Fellowship.

References

[1] Anderson, C., *A vortex method for flows with slight density variations,* J. Comput. Phys., 61, 1985, pp.417–444.

[2] Anderson, C., and Greengard, C., *On vortex methods,* SIAM J. Numer. Anal., 22, 1985, pp. 413–440.

[3] Ashurst, W.T., and Meiron, D.I., *Numerical study of vortex reconnection,* Phys. Rev. Lett., 58, 1987, pp.1632–1635.

[4] Beale, J.T., *A convergent 3-d vortex method with grid free stretching,* Math. Comp., 46, 1986, pp.401–424.

[5] Beale, J.T., Kato, T., and Majda, A., *Remarks on the breakdown of smooth solutions for the Euler equations,,* Comm. Math. Phys., 94, 1984, pp.61–66.

[6] Beale, J.T., and Majda, A., *Rates of convergence for viscous splitting of the Navier-Stokes equations,* Math. Comp., 37, 1981, pp.243–259.

[7] Beale, J.T., and Majda, A., *Vortex methods I : convergence in three dimensions,* Math. Comp., 39, 1982, pp.1–27.

[8] Beale, J.T., and Majda, A., *Vortex methods II : higher order accuracy in two and three Dimensions,* Math. Comp., 39, 1982, pp.29–52.

[9] Chorin, A.J., *Vortex models and boundary layer instability,* SIAM J. Sci. Stat. Comput., 1, 1980, pp.1–24.

[10] Chorin, A.J., *The evolution of a turbulent vortex,* Commun. Math. Phys., 83, 1982, pp.517–535.

[11] Chorin, A.J., *Turbulence and vortex stretching on a lattice,* Comm. Pure App. Math., 39, 1986, pp.S47–S65.

[12] Greengard, C., *Convergence of the vortex filament method,* Math. Comp., 47, 1986, pp.387–398.

[13] Kambe, T. and Takao, T., *Motion of distorted vortex rings, Jour. Phys. Soc. Japan,* **31**, 591–596.

[14] Krasny, R., *Desingularization of periodic vortex sheet roll-up,* J. Comput. Phys., 65, 1986, pp.292–313.

[15] Leonard, A., *Computing three-dimensional incompressible flows with vortex elements,* Annual Rev. Fluid Mech., 17, 1985, pp.523–559.

[16] Melander, M.V., and Zabusky, N.J., *Interaction and reconnection of vortex tubes via direct numerical simulations,* Proceedings IUTAM Symposium on Fundamental Aspects of Vortex Motion, Aug. 31 - Sept. 4, 1987, Tokyo, Japan.

[17] Pumir, A., and Kerr, R.M., *Numerical simulation of interacting vortex tubes,* Phys. Rev. Lett., 58, 1987, pp.1636–1639.

[18] Schatzle, P., *An experimental study of fusion of vortex rings,* Ph. D. Thesis, California Institute of Technology, 1987.

[19] Siggia, E.D., *Collapse and amplification of a vortex filamnet,* Phys. Fluids, 28, 1985, pp.794–805.

[20] Siggia, E.D., and Pumir, A., *Incipient singularities in the Navier-Stokes equations,* Phys. Rev. Lett., 55, 1985, pp.1749–1752.

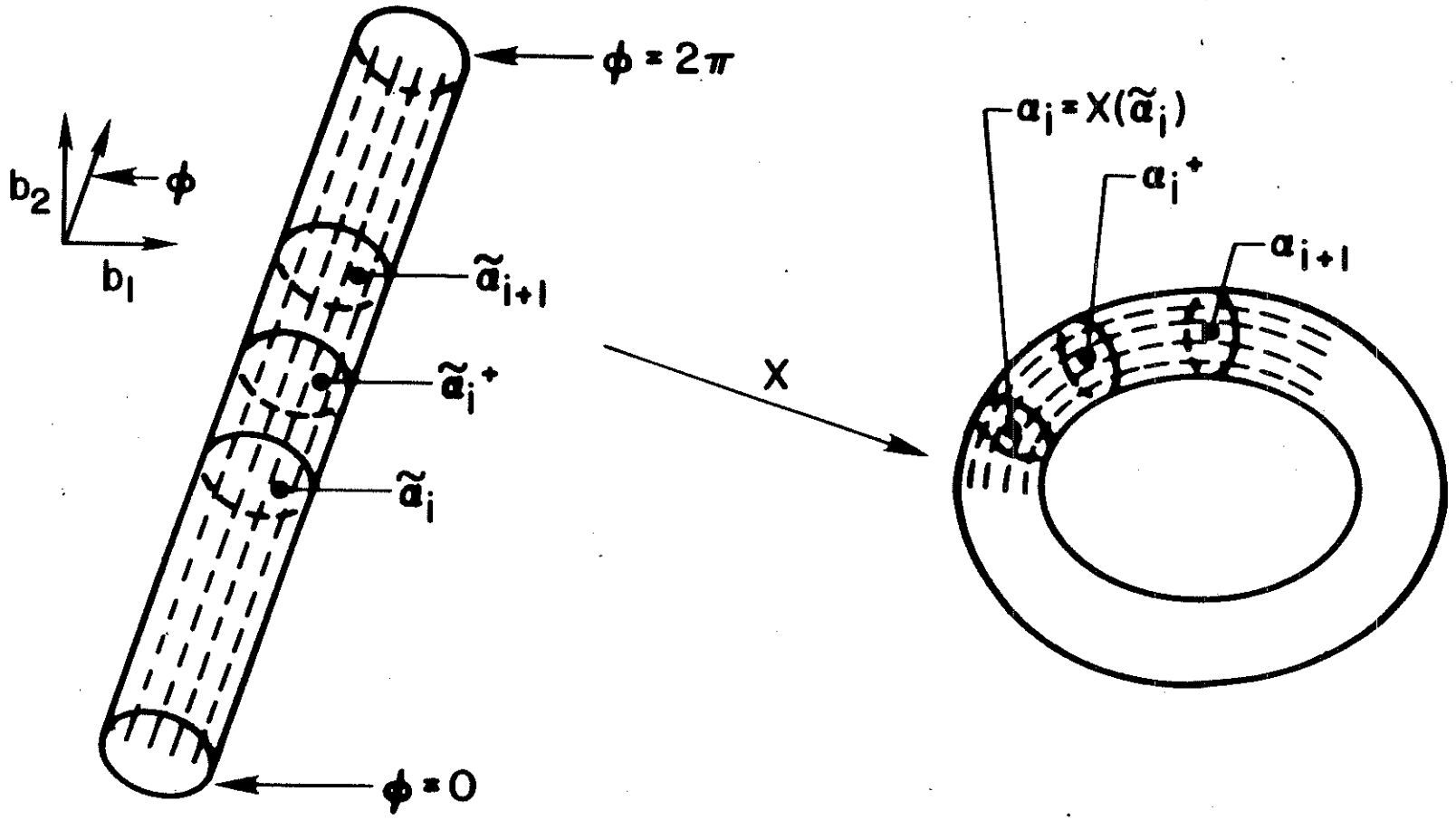

Figure 1.

Discrete Parameterization of Vortex Ring

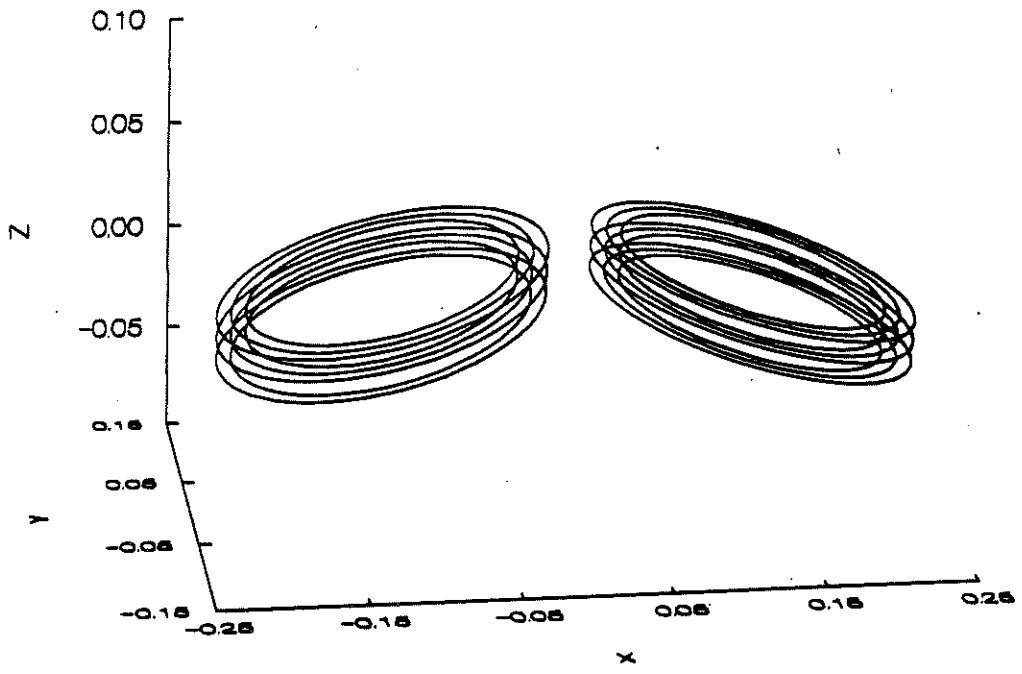

Figure 2

Initial Vortex Ring Configuration

3(A)

3(B)

3(C)

3(D)

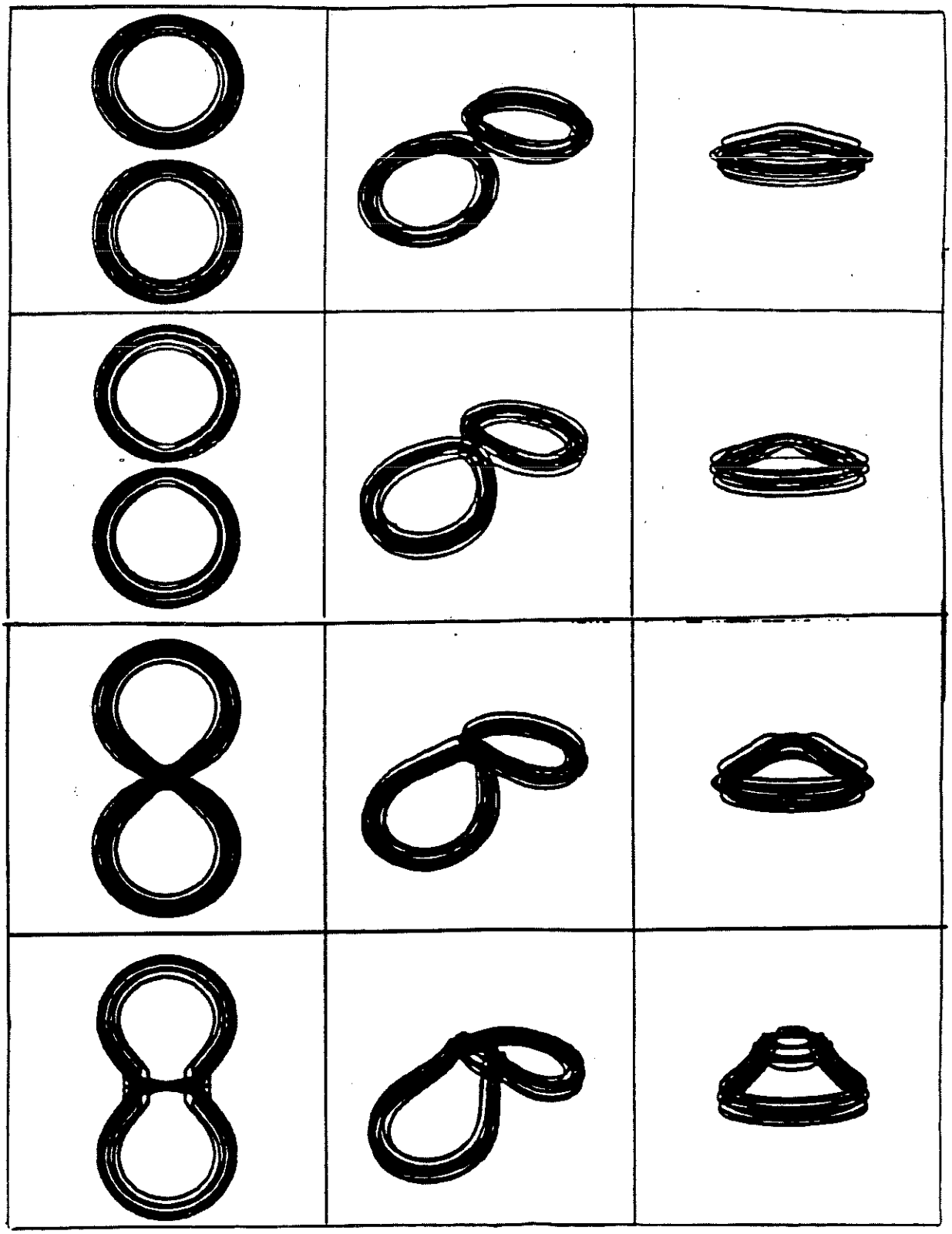

Figure 3

Perspective Views of Vortex Rings

Rows (A) - (D) are the results for steps 16, 32, 48 and 64. The first column is a top view of the rings. The view is along the z axis. The second column is a corner view of the rings along the vector $(1, 1, \frac{1}{2})$. The third column is an end view. The view is along the x axis and the ring on the far side is deleted for clarity. In this computation $\delta = .012$.

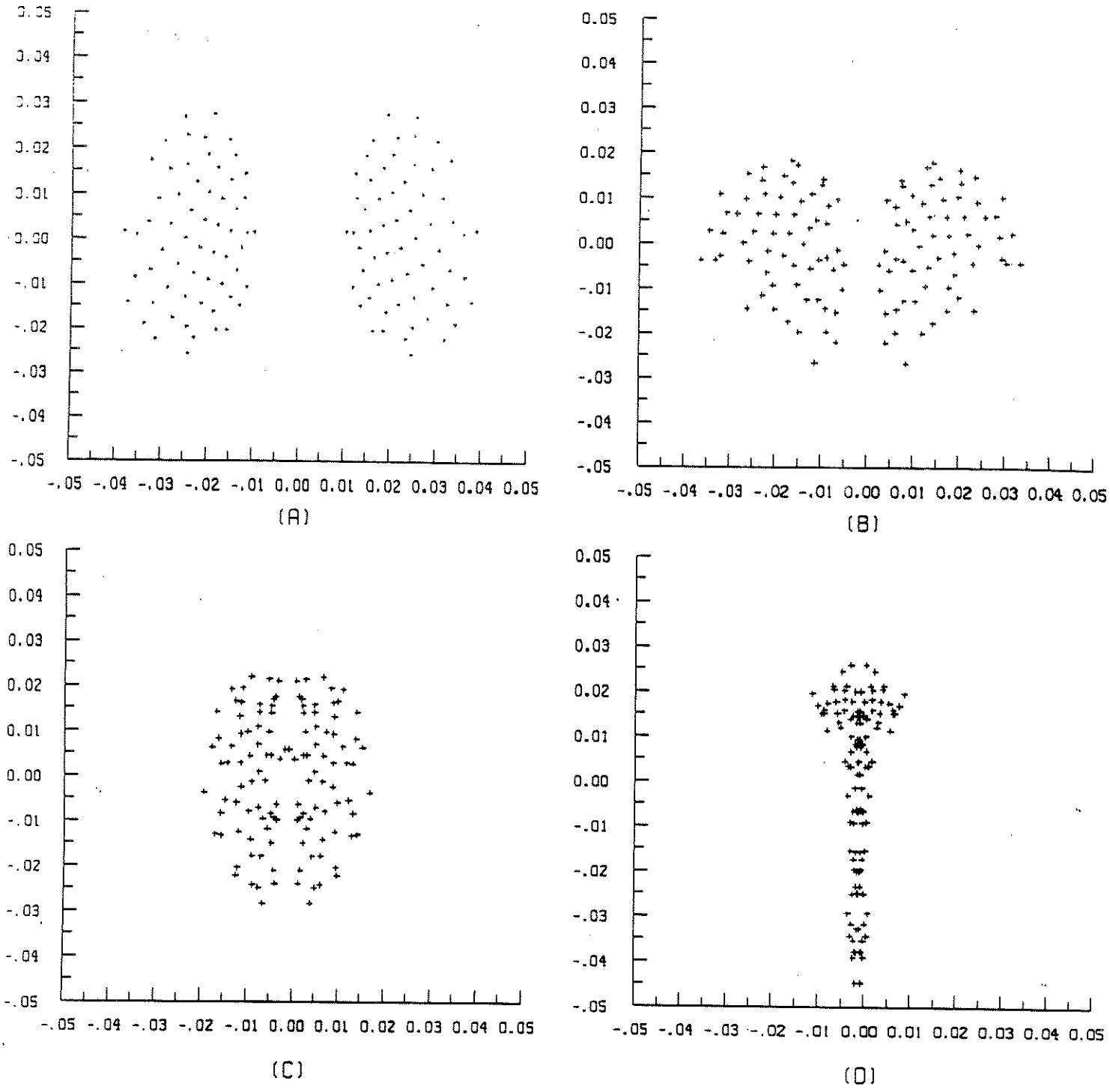

Figure 4

Vortex Core Cross-Sections

$\delta = .012$

(A) - Step 16 (B) - Step 32 (C) - Step 48 (D) - Step 64

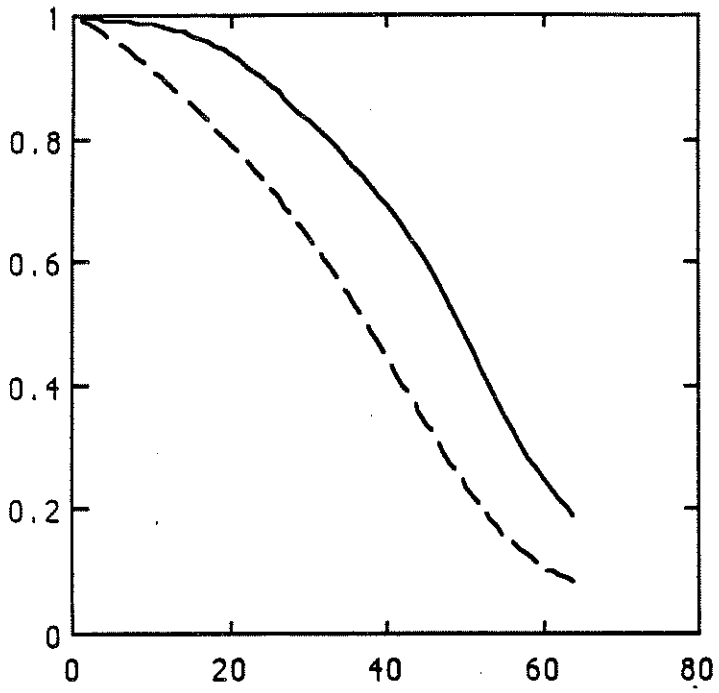

Figure 5(a)

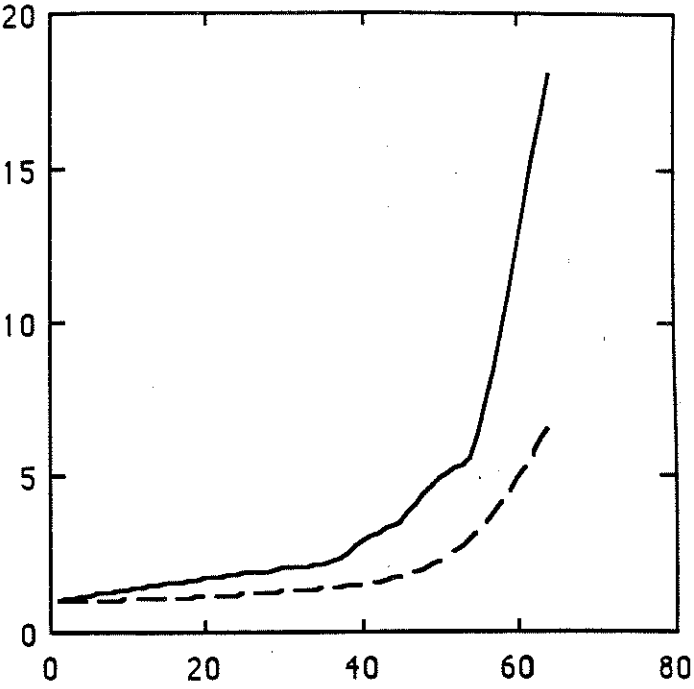

Figure 5(b)

——— : relative x location of vortex core

- - - : relative core cross-sectional area

——— : maximum relative stretching

- - - : average relative stretching

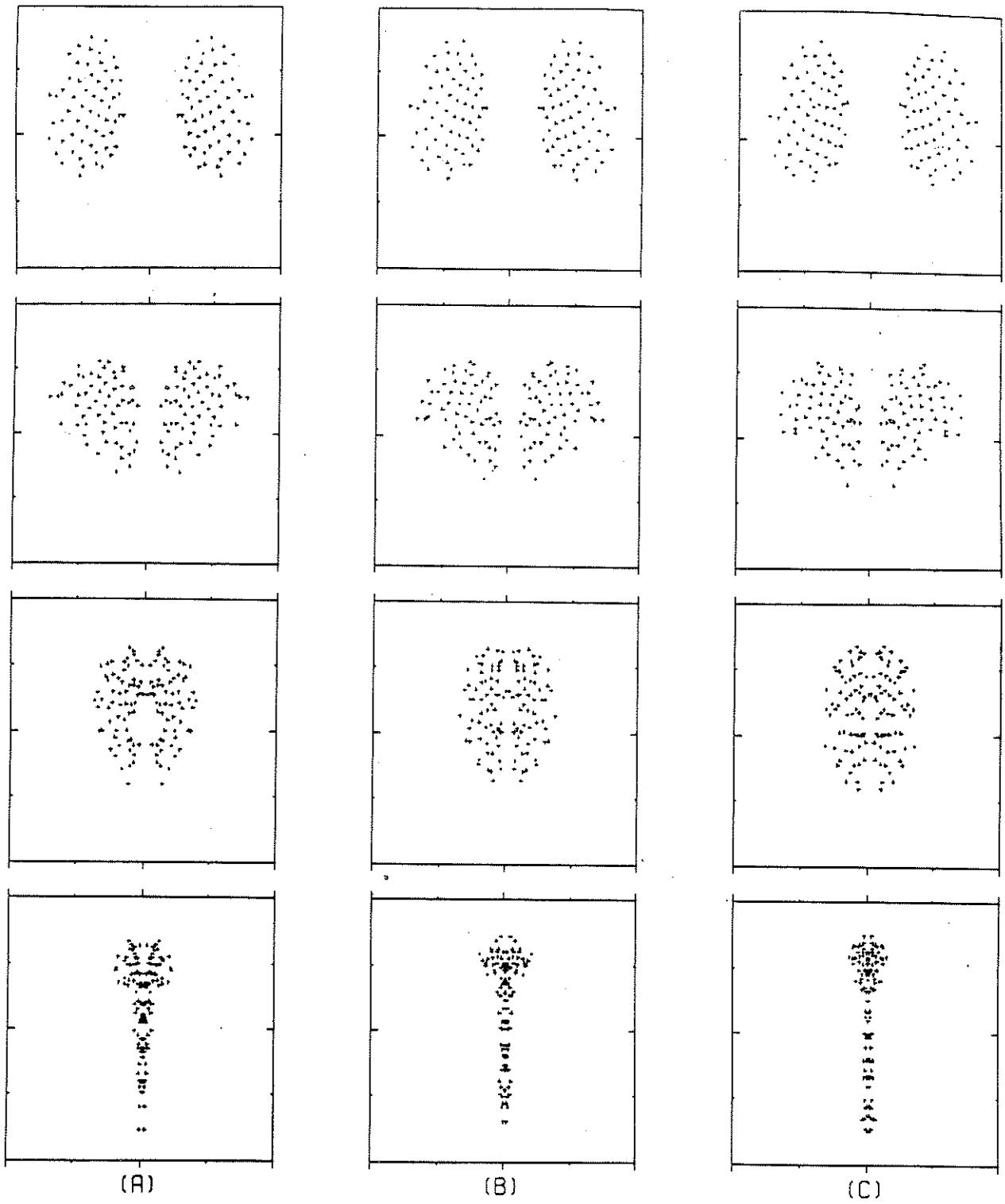

Figure 6

Vortex Core Cross-Sections

(A) : ϵ=.015, Steps 16,32,48,64

(B) : ϵ=.012, Steps 16,32,48,64

(C) : ϵ=.010, Steps 16,32,48,64

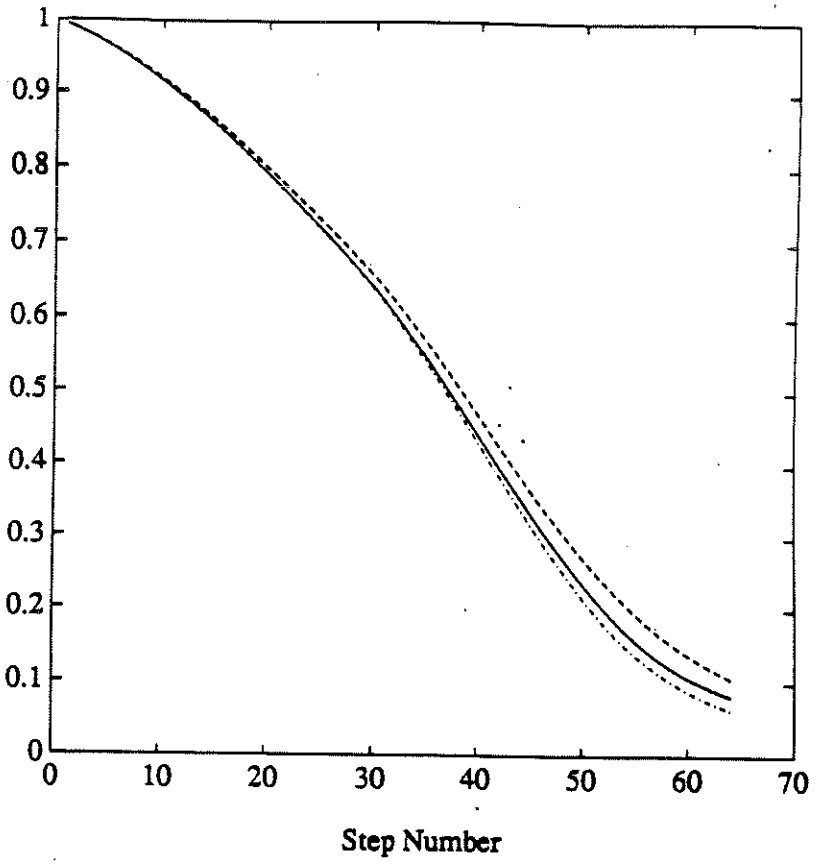

Figure 7

_ _ _ _ : relative core distance $\epsilon = .015$

_____ : relative core distance $\epsilon = .012$

_ . _ . _ : relative core distance $\epsilon = .010$